Journal of Applied Physics ARTICLE scitation.org/journal/jap

Strong thermal conductivity dependence on arsenic-vacancy complex formation in arsenic-doped silicon

Cite as: J. Appl. Phys. **126**, 195104 (2019); doi: 10.1063/1.5126160
Submitted: 30 August 2019 · Accepted: 5 November 2019 ·
Published Online: 19 November 2019

Yongjin Lee[a] and Gyeong S. Hwang[b]

AFFILIATIONS

McKetta Department of Chemical Engineering, University of Texas at Austin, Austin, Texas 78712, USA

[a]**Present address:** School of Physical Science and Technology, ShanghaiTech University, Shanghai 201210, China.
[b]**Author to whom correspondence should be addressed:** gshwang@che.utexas.edu

ABSTRACT

High-concentration doping of silicon (Si)-based materials is an effective way to improve their thermoelectric efficiency via thermal conductivity (κ) reduction as well as thermopower and electrical conductivity enhancement. Beyond the solubility limit, a large portion of dopant atoms may undergo clustering mediated primarily by point defects, which may in turn significantly alter the physical properties of host materials. In this work, we investigate the effect of Arsenic-vacancy (AsV) complex formation on κ in heavily As-doped Si using molecular dynamics simulations. The simulation results clearly demonstrate that the presence of AsV complexes, particularly As_4V which is the most stable one, may result in a substantially lower κ compared to the case where all As atoms remain substitutional and electrically active. Further analysis reveals that the central vacancy in As_4V causes Si lattice softening and thus results in the reduction of phonon group velocity. Our findings highlight the significant effect of dopant clustering on κ and also provide some guidance on how to manipulate Si-based materials to improve their thermoelectric performance via doping combined with defect engineering.

I. INTRODUCTION

Silicon (Si)-based nanomaterials have been extensively investigated for thermoelectric (TE) applications largely because Si is naturally abundant, cheap, and environmentally friendly, and it also has well-established processing techniques.[1,2] Due to its high thermal conductivity (κ), bulk crystalline Si (*c*-Si) is considered a poor TE material with a figure of merit of $ZT \sim 0.01$ at room temperature.[3] Therefore, significant research efforts[4–7] have been directed toward exploring the most effective way to reduce κ in Si while maintaining electrical conductivity (σ). Besides nanostructuring and alloying,[8–10] incorporation of heavier or lighter dopant atoms into Si has been proven to be an effective means of suppressing κ through increase primarily in the mass disorder-induced scattering. Previous studies[11,12] have reported the reduction of κ by a factor as large as 20 for substitutionally doped *c*-Si at concentrations on the order of 10^{20} atoms/cm^3.

Arsenic (As) is the most common n-type dopant used in Si-based devices, by virtue of its high solubility[13] and rather low diffusivity.[13,14] The heteroatom can be incorporated into Si beyond its solubility limit using low energy ion implantation followed by high-temperature annealing. During the process, As atoms may undergo defect-mediated diffusion and agglomeration. In highly As-doped Si, the concentration of free electrons tends to saturate at the level of approximately 2×10^{20} cm^{-3}.[15] Previous studies[16–19] have identified the formation of stable As-vacancy complexes, such as As_3V, As_4V, As_2V_2, and As_3V_2 (where V indicates a vacancy), which may play a major role in As deactivation. The presence of dopant-defect clusters could be expected to significantly alter the physical properties of the host material. It has also been reported that highly doped Si (>5×10^{20} cm^{-3}) shows promise as a TE material, in which dopant atoms possibly segregated at grain boundaries and interfaces might affect its TE properties.[20,21] At such high dopant concentrations, we could also expect the formation of large concentrations of dopant-defect clusters in bulk Si. Thus far, however, little is yet known about the effect of dopant-defect clustering on thermal transport in Si, despite its importance in guiding how to manipulate Si-based materials to achieve desired TE properties through doping combined with defect engineering.

In this work, we employ both equilibrium and nonequilibrium molecular dynamics (EMD and NEMD) simulations to investigate the effects of As-vacancy complex formation on the κ of As-doped Si. Our focus is placed on As_4V, which is the most stable complex, that consists of a central vacancy and four surrounding As atoms.[16] The interatomic interactions for As_4V are described using Stillinger-Weber (SW) potential parameters that we reoptimize based on the first-principles-based force-matching method.[22] Variations in κ with dopant concentration and relative As_4V content are evaluated using EMD and NEMD simulations. Further analysis is also performed to clarify the mechanisms underlying the contribution of As-vacancy clusters to the reduction of κ.

II. COMPUTATIONAL DETAILS

All MD simulations reported herein were performed with a 1 fs time step. A detailed description of the simulation procedure can be found in our previous work.[23] As shown in Fig. 1, the simulation box was subdivided into thin slabs consisting of a heat source (S_H) layer, a heat sink (S_C) layer, two intermediate (I) layers, and two buffer (B) layers. We employed a composite cell scheme with the cross section of the simulation box consisting of 10×10 units (corresponding to 400 atoms). The S_H/S_C and B layer thicknesses were set at respective L_S and L_B values corresponding to one (or 400 atoms) and ten (or 4000 atoms) units, respectively, in the axial ⟨100⟩ direction. The intermediate layer thickness L_I was varied from 40, 80, and 120 to 160 units (corresponding to 16 000, 32 000, 64 000, and 128 000 atoms) depending on the total simulation cell length (L_{tot}). As_4V complexes were randomly distributed throughout the simulation domain in an isolated manner without cluster overlaps. Furthermore, the dopant concentrations in the S_H/S_C, B, and I layers were controlled to be (nearly) equal. Periodic boundary conditions were imposed in the x, y, and z directions, with heat conduction in the z direction.

A temperature gradient (ΔT) (in the direction of the flow) was obtained from an imposed heat flux (J) to determine the value of κ ($=-J/\Delta T$) as described by the Müller-Plathe method.[24] The bulk κ values were obtained through extrapolation of a discretized range of finite-size results. For a given simulation-cell-size and dopant-concentration system, we performed 25 independent NEMD simulations considering 5 different atomic-level spatial distributions of dopants, for each of which 5 different initial velocity distributions were taken into account. For quantum correction,[25] doped Si systems considered were assumed to have the same T_D as Si where $T_D(\text{Si}) = 645$ K,[26] as the atomic fractions of dopants are very small (<0.015). The thermal conductivities of As_4V-doped Si systems were calculated using NEMD with the SW potential model at various doping concentrations at 300 K. To compare the impurity scattering strengths between substitutional As-doped and As_4V-doped Si, the κ values for point As-doped bulk c-Si were calculated at corresponding concentrations. To model the interactions of substitutional As and Si, we adopted parameter set from our previous work also obtained using force field matching.[11]

For MD simulations performed using LAMMPS,[27] we employed a general form of SW potential function equipped with optimized SW parameters for Si-As interactions in As_4V-doped Si that were obtained using a force-matching method[22] based on density functional theory (DFT) calculations. The inset of Fig. 2 shows a schematic view of the As_4V complex fully relaxed using DFT, with important geometric information. The DFT force data for the parameter optimization was obtained using a 63-atom cubic supercell (one As_4V complex + 59 Si atoms) by displacing As atoms or its neighboring Si atoms by 0.08 Å in the x, y, and z directions. All DFT calculations were performed within the Perdew-Wang generalized gradient approximation (GGA-PW91)[28] as implemented in the Vienna *Ab initio* Simulation Package (VASP).[29] The restoring forces acting on the displaced atom and its first-nearest neighbors were considered to be matched in the SW parameter adjustments. Table I summarizes the modified parameters for the As_4V complex from the force

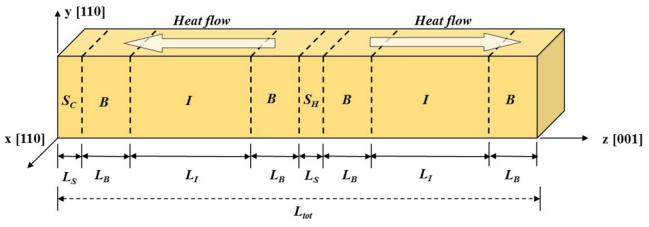

FIG. 1. A schematic of a rectangular-shaped simulation domain. Periodic boundary conditions are imposed in the x, y, and z directions. The simulation cell consists of heat source (S_H), two heat sink (S_C), four buffer (B), and two intermediate (I) layers. For thermal conductivity calculation, temperature gradients in the I layers were used to avoid any undesired effects that arise from velocity swapping-induced nonphysical phonon scatterings in the S_H and S_C regions. Heat transfer is in two directions that are + z and – z due to the periodic boundary condition imposed in the [001] direction.

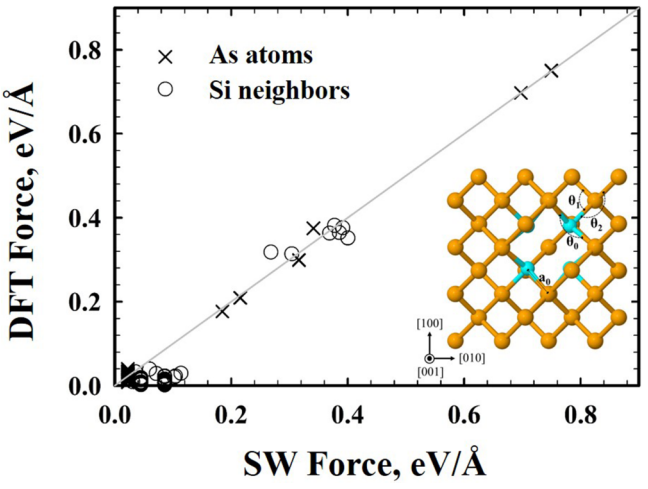

FIG. 2. Comparison between DFT and SW forces acting on one of the four As atoms (surrounding a vacancy), which is slightly displaced, and its three first-nearest Si atoms in As_4V. The solid line indicates |SW Force–DFT Force| = 0. The inset shows a schematic view of the As_4V complex in c-Si, where $a_0 = 2.436$ Å, $\theta_0 = 103.5°$, $\theta_1 = 106.5°$, and $\theta_2 = 115.7°$. The orange and cyan balls represent Si and As atoms, respectively.

TABLE I. Modified parameters of the Stillinger-Weber interatomic potential for Si-As interactions for As_4V; here, σ, ε, λ, *a*, and $\cos\theta_0$ values are based on fit to DFT-GGA calculations. Note that no As-As covalent bond exists in As_4V.

	Si-As		
σ	2.1702		
ε (eV)	1.2451		
λ	39.4445		
a	1.7717		
	Si-As-Si	As-Si-Si	
$\cos\theta_0$	−0.2337	−0.2835	−0.4340
	$A = 7.049556277$, $B = 0.6022245584$, $p = 4.0$, $q = 0.0$, and $\gamma = 1.0$		

matching approach. The σ value was chosen to match the Si-As bond distances from DFT-GGA calculations. In addition, the equilibrium Si-As-Si bond angles (θ_0) were obtained from DFT-GGA calculations. For the substitutional As dopant, Si-Si-As bond angles retained as 109.47° (= the bond angle for Si diamond structure). The formation of the As_4V complex, however, introduces significant lattice distortions to neighboring Si atoms. To take this into account, two equilibrium Si-Si-As bond angles (106.47° and 115.73°) from the DFT calculations were employed. Figure 2 shows the comparisons of the restoring forces from our SW and DFT- GGA calculations; overall, the modified SW parameters provide a highly accurate reproduction of the corresponding DFT forces (acting on As atoms and their Si neighbors) for the As_4V-doped system.

III. RESULTS AND DISCUSSION

The effect of As_4V formation on the κ of As-doped *c*-Si was evaluated through comparison of two different systems that contain either As_4V clusters (hereafter referred to as "aggregated") or singly dispersed substitutional As atoms ("dispersed"). Figure 3 shows predicted thermal conductivities for the aggregated (κ_{As4V}) and dispersed (κ_{As}) systems, respectively, with varying concentrations of As ($n_{As} = 1.22$, 2.44, 4.88, and 7.31×10^{20} cm^{-3}, corresponding to atomic percentages of $x_{As} = 0.25$, 0.5, 1, and 1.5 at. %, respectively, with respect to 5×10^{22} atoms/cm^3 in *c*-Si). The results clearly demonstrate that κ_{As4V} decreases more rapidly than κ_{As}, indicating that the dependence of κ on n_{As} will become stronger as As atoms aggregate to form As_4V clusters. Moreover, the monotonic decrease in the ratio of $\kappa_{As4V}/\kappa_{As}$ with n_{As}, as shown in Fig. 4, suggests that the impact of As_4V formation will become greater as n_{As} increases.

The predicted κ values are well fitted by the inverse power-law relationship $\kappa = \kappa_{Si}/(1 + A\bar{n}_{As}^{\alpha})$, where κ_{Si} is the thermal conductivity of undoped *c*-Si at 300 K ($\kappa_{Si} = 136.65$ W m^{-1} K^{-1}) taken from our previous work,[22] $\bar{n}_{As}$ is the dimensionless As concentration (= $n_{As}/10^{20}$ cm^{-3}), and A and α are adjustable parameters. This relationship has been widely adopted to describe the reduction of κ due to phonon scattering by pointlike defects and impurities.[23,30–32] The best fit is obtained with parameters $A = 2.11$ (1.35) and $\alpha = 1.04$ (0.94) for the aggregated (dispersed) system; the larger values of A and α are indicative of stronger dependence of κ on n_{As}. From the power-law equations, κ_{As4V} and κ_{As} are approximated to be 8% and 14% of κ_{Si}, respectively, at $x_{As} = 1$ at. %, and they are further reduced to 1.6% and 3.4% of κ_{Si}, respectively, as x_{As} increases to 5 at. %. The respective $\kappa_{As4V}/\kappa_{As}$ are 0.58 and 0.47 when $x_{As} = 1$ at. % and 5 at. %; the substantially reduced κ highlights the importance of considering As-vacancy clustering in predicting thermal transport in highly As-doped *c*-Si.

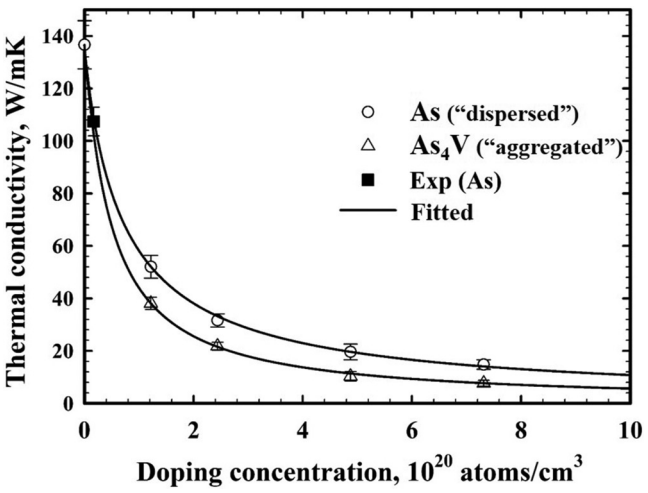

FIG. 3. Predicted bulk thermal conductivities for As doped c-Si with either As_4V ("aggregated") or substitutional As ("dispersed") at 300 K as a function of As dopant concentration (n_{As}), together with an available experimental value for comparison. The solid line indicates a fitted curve to the predicted values with $R^2 = 0.99$, which is $\kappa = \kappa_{Si}/[1 + A(n_{As}/10^{20})^{\alpha}]$ with $\kappa_{Si} = 136.65$ W m^{-1}K^{-1}.

We attribute further reduction of κ associated with As_4V formation primarily to the presence of a single vacancy in As_4V,

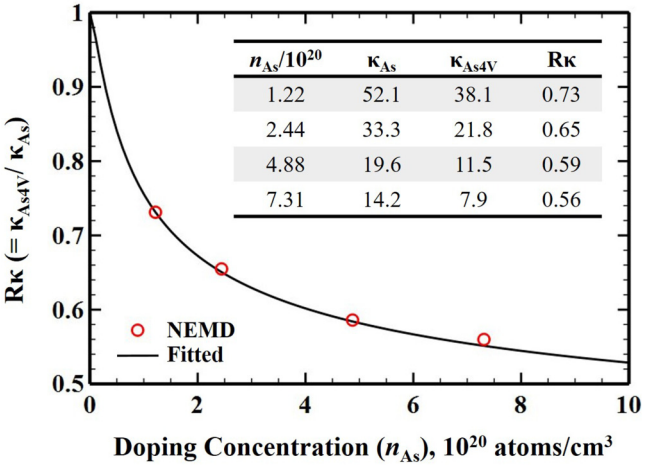

$n_{As}/10^{20}$	κ_{As}	κ_{As4V}	Rκ
1.22	52.1	38.1	0.73
2.44	33.3	21.8	0.65
4.88	19.6	11.5	0.59
7.31	14.2	7.9	0.56

FIG. 4. Ratios of the thermal conductivity values for the "aggregated" and "dispersed" systems, $R_\kappa = \kappa_{As4V}/\kappa_{As}$, from NEMD simulations (open circles) and inverse power-law fitting with $R^2 = 0.99$ ("solid line"), respectively, as presented in Fig. 3.

which may cause stronger phonon scattering as compared to the case of only As substitution. To confirm this, we evaluated the sole contribution of dopant aggregation associated with the mass disorder; here, the vacancy in As_4V is filled with Si (i.e., As_4Si in which one Si atom is surrounded by four As atoms) to exclude the vacancy effect. The mass-disorder effect was evaluated by setting the radius and force constants of As to equal those of Si, while retaining their respective masses ($m_{As} = 74.92$ and $m_{Si} = 28.08$). At $n_{As} = 4.88 \times 10^{20}$ cm^{-3}, the κ are predicted to be 21.2 W m^{-1} K^{-1} for the case of As_4Si, which is higher than 19.6 W m^{-1} K^{-1} for the dispersed case. This suggests that the dispersed case can be more effective in suppressing κ, which is not surprising considering that it gives a larger number of scattering centers than the aggregated case. However, the difference in the effect of mass disorder due to As aggregation appears to be marginal particularly when n_{As} is relatively high, as evidenced by the small difference of 1.6 W m^{-1} K^{-1} between the dispersed and aggregated cases. We also assessed the aggregation-induced difference in the bond-disorder effect considering As_4Si, instead of As_4V, to exclude the vacancy effect. Here, the mass and radii values of As are set equal to those of Si, while maintaining the optimized force constants for each system. Similar to the mass-disorder case, the dispersed system is found to have a lower κ (=52.3 W m^{-1}K^{-1}) compared to the agglomerated system (κ = 58.1 W m^{-1} K^{-1}).

Our analysis shows that aggregation of As atoms, with no vacancy creation, may reduce the associated mass-disorder and bond-disorder effects, leading to being less effective in suppressing κ; such dopant aggregation effects are predicted to be marginal, particularly when the host material is heavily doped. However, as mentioned earlier, As aggregates may further be stabilized by forming As_4V or other vacancy-containing complexes. To demonstrate the vacancy effect, we calculated the κ of *c*-Si with single vacancies; in fact, vacancies in Si are known to be highly mobile such that they may mostly remain in the form of clusters at finite temperatures.[33–35] Nonetheless, the model calculation would be reasonable enough to approximate the effect of vacancy scattering on the reduction of κ. At a vacancy concentration of $n_V = 1.22 \times 10^{20}$ cm^{-3}, the predicted κ is reduced to 25% of κ_{Si}, which is much lower than about 38% of κ_{Si} for the dispersed system at $n_{As} = 1.22 \times 10^{20}$ cm^{-3}, clearly demonstrating the stronger effect of vacancies than As dopants. This implies that creation of single (or small) vacancies surrounded by As atoms could play an important role in determining the κ of As-doped *c*-Si.

Further analysis was performed to clarify the mechanisms underlying the effect of As_4V formation on the reduction of κ. We calculated and compared the contributions of individual phonon modes to κ in the dispersed and aggregated systems, using the Boltzmann transport equation (BTE)-relaxation time approximation (RTA) method based on time-domain normal mode analysis (TDNMA)[36–38] extracted from a combination of EMD trajectories and anharmonic lattice dynamics. Figure 5 shows the accumulated κ with the phonon frequency ω at $n_{As} = 4.88 \times 10^{20}$ cm^{-3} (corresponding to $x_{As} \approx 0.01$) and $T = 300$ K. The accumulation of κ tends to saturate beyond 3 THz, implying that the heat is predominantly carried by low-frequency (ω < 3 THz) phonons in these samples. Note also that the accumulated κ begins to show a distinctive difference between the aggregated and dispersed cases

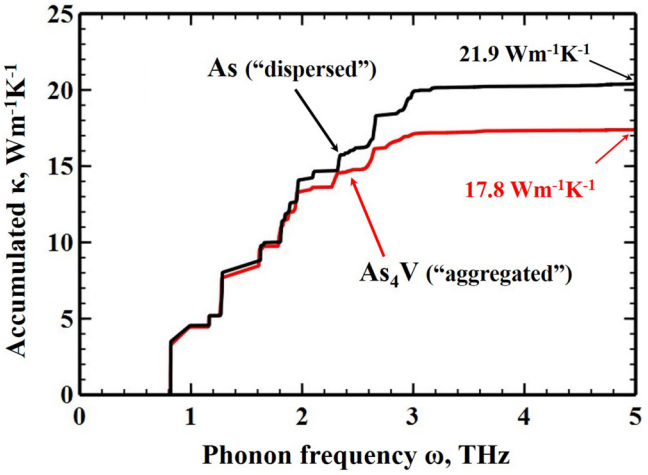

FIG. 5. Comparison of the accumulated thermal conductivity (κ) with respect to the phonon frequency (ω) at $n_{As} = 4.88 \times 10^{20}$ cm^{-3} for the aggregated (As_4V) and dispersed (As) cases using the BTE-RTA method based on time-domain normal mode analysis from EMD trajectories.

when ω ≈ 2 THz; this suggests that the increased scattering of phonons with frequencies between 2 and 3 THz could be mainly responsible for the relatively lower κ of the aggregated system. We also find that our BTE-RTA results somewhat overestimate κ compared to our NEMD predictions in Fig. 3. A major source of these discrepancies could be the neglect of possible collective excitations under the single-mode relaxation time approximation, in addition to the relatively smaller system size employed in TDNMA. Nonetheless, our TDNMA demonstrates that the thermal transport properties of As-doped *c*-Si can be substantially affected by the formation of As-vacancy clusters.

According to kinetic theory, the κ can be described phenomenologically in terms of heat capacity *C*, phonon group velocity v_g, and mean free path *l* (or phonon lifetime τ), i.e., $\kappa \propto Cv_gl$ (= $Cv_g^2\tau$). We estimated v_g and τ at 300 K, while *C* could be expected to be relatively insensitive to As_4V formation. As summarized in Fig. 6(a), while there is a rapid drop in τ for both the aggregated and dispersed systems, τ tends to be relatively longer in the former in the low-frequency region considered. This could be attributed to the smaller number of scattering centers, as discussed earlier, which results in a shorter *l* for phonons to travel; note that τ represents the average traveling time between collisions of phonon modes. It would be also worth noting that the dependence of τ on ω appears slightly weaker than the typical scaling, $\tau \propto \omega^{-2}$, for bulk *c*-Si where three-phonon umklapp scattering is dominant.

Figure 6(b) shows a comparison of calculated v_g in between the aggregated and dispersed systems. Overall, v_g in the aggregated system appears to be smaller relative to those in the dispersed system; especially, the difference of v_g is quite noticeable when ω = 2–3 THz (where there is a distinct difference in κ accumulation, as shown in Fig. 5). This analysis suggests that the smaller v_g arising from strong vacancy-phonon scattering at low ω (<3 THz)

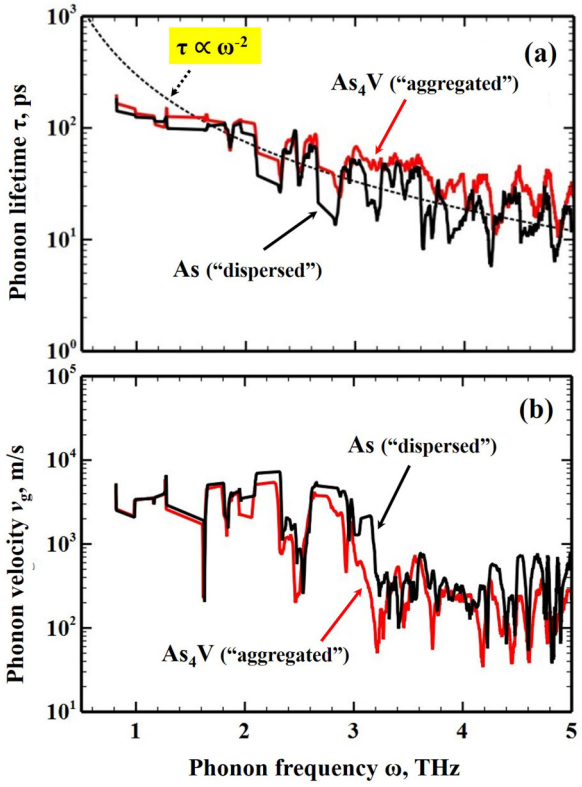

FIG. 6. Comparisons of (a) phonon lifetime, τ, and (b) phonon group velocity, v_g, between the aggregated (As_4V) and dispersed (As) systems at $n_{As} = 4.88 \times 10^{20}\,cm^{-3}$.

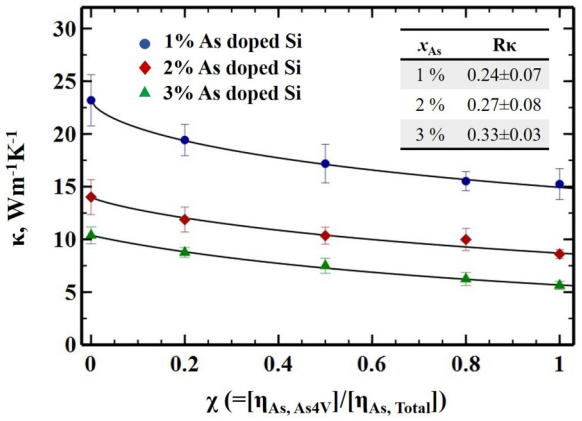

FIG. 7. Variations in thermal conductivity (κ) for As doped *c*-Si, from EMD simulations at 300 K, with the fraction of As atoms in As_4V complexes [χ = (number of As atoms in As_4V)/(total number of As atoms)] at three different As atomic percentages (x_{As} = 1, 2, and 3 at. %, as indicated). The inset table shows the ratio R_κ ($=\kappa_{As4V}/\kappa_{As}\kappa_{As}$) of the fully "aggregated" and "dispersed" systems.

can be primarily responsible for the greater reduction of κ in the aggregated system compared to the dispersed system.

Finally, EMD simulations were performed to calculate the variation of κ with As_4V content for systems containing both As_4V clusters and isolated substitutional As atoms at $x_{As} = 1$, 2, and 3 at. % (corresponding $n_{As} = 0.5 \times 10^{21}$, 1.0×10^{21}, and $1.5 \times 10^{21}\,cm^{-3}$). At each x_{As}, the relative As_4V content [χ = fraction of As atoms in As_4V = (number of As atoms in As_4V)/(total number of As atoms)] was varied from 0.0, 0.2, 0.5, 0.8 to 1.0]. The results are summarized in Fig. 7. For each system, five independent samples were considered. Overall, the predicted κ by EMD tends to be greater than those by NEMD (in Fig. 3). Nonetheless, our results show a clear trend that κ monotonically decreases as χ increases for all x_{As} considered. Considering that the formation of As-vacancy clusters becomes more probable with increasing x_{As}, the thermal transport properties of heavily As-doped *c*-Si can be sensitive to sample preparation processes and conditions by which their relative concentrations will be determined. While our work highlights the important role played by dopant-defect clusters, the finding may open up the possibility to control the κ of *c*-Si through utilization of the synergistic contributions of doping and defect engineering.

IV. CONCLUSIONS

Molecular dynamics (MD) simulations were employed to investigate the effect of As_4V complex formation on phonon scattering and thermal conductivity in As doped Si with varying total dopant concentrations and relative As_4V contents. The Stillinger-Weber potential parameters used for Si-As interactions were reoptimized by fitting to first-principles calculation results. The simulation results clearly demonstrate that the κ of As doped Si monotonically decreases with increasing the As_4V content, as compared to the case where substitutional As atoms are fully dispersed. Our analysis clarifies that further reduction in κ is largely attributed to the "lattice softening" caused by the single vacancy surrounded by four As atoms in As_4V that leads to a reduced phonon velocity. This work highlights the critical role of dopant-defect clusters in determining the thermal transport properties of heavily doped Si, which would further open up the possibility to realize highly efficient Si-based TE materials via controlled doping and defect engineering.

ACKNOWLEDGMENTS

This work was supported in part by the Robert A. Welch Foundation (No. F-1535). Y. Lee is grateful for the scholarship from the Donald D. Harrington Fellows Program. We also thank the Texas Advanced Computing Center for the use of their computing resources.

REFERENCES

[1]R. Venkatasubramanian, E. Siivola, T. Colpitts, and B. O'Quinn, Nature **413**, 597 (2001).
[2]B. Poudel, Q. Hao, Y. Ma, Y. Lan, A. Minnich, B. Yu, X. Yan, D. Wang, A. Muto, D. Vashaee, X. Chen, J. Liu, M. S. Dresselhaus, G. Chen, and Z. Ren, Science **320**, 634 (2008).
[3]L. Weber and E. Gmelin, Appl. Phys. A **53**, 136 (1991).
[4]W. Liu and M. Asheghi, J. Appl. Phys. **98**, 123523 (2005).

[5]M. Asheghi, K. Kurabayashi, R. Kasnavi, and K. E. Goodson, J. Appl. Phys. **91**, 5079 (2002).
[6]M. E. Brinson and W. Dunstant, J. Phys. C: Solid State Phys. **3**, 483 (1970).
[7]A. D. McConnell, S. Uma, and K. E. Goodson, J. Microelectromech. Syst. **10**, 360 (2001).
[8]I. Ponomareva, D. Srivastava, and M. Menon, Nano Lett. **7**, 1155 (2007).
[9]A. Skye and P. K. Schelling, J. Appl. Phys. **103**, 113524 (2008).
[10]T. M. Gibbons, B. Kang, S. K. Estreicher, and C. Carbogno, Phys. Rev. B **84**, 035317 (2011).
[11]Y. Lee and G. S. Hwang, Phys. Rev. B **86**, 075202 (2012).
[12]G. A. Slack, J. Appl. Phys. **35**, 3460 (1964).
[13]R. Angelucci, J. Electrochem. Soc. **132**, 2726 (1985).
[14]P. M. Fahey, P. B. Griffin, and J. D. Plummer, Rev. Mod. Phys. **61**, 289 (1989).
[15]P. M. Rousseau, P. B. Griffin, W. T. Fang, and J. D. Plummer, J. Appl. Phys. **84**, 3593 (1998).
[16]K. C. Pandey, A. Erbil, G. S. Cargill, R. F. Boehme, and D. Vanderbilt, Phys. Rev. Lett. **61**, 1282 (1988).
[17]M. Ramamoorthy and S. T. Pantelides, Phys. Rev. Lett. **76**, 4753 (1996).
[18]V. Ranki, K. Saarinen, J. Fage-Pedersen, J. L. Hansen, and A. N. Larsen, Phys. Rev. B **67**, 041201 (2003).
[19]S. A. Harrison, T. F. Edgar, and G. S. Hwang, Electrochem. Solid-State Lett. **9**, G354 (2006).
[20]N. Uchida, T. Tada, Y. Ohishi, Y. Miyazaki, K. Kurosaki, and S. Yamanaka, J. Appl. Phys. **114**, 134311 (2013).
[21]E. Acosta, V. Smirnov, P. S. B. Szabo, J. Buckman, and N. S. Bennett, J. Electron. Mater. **48**, 2085 (2019).
[22]Y. Lee and G. S. Hwang, Phys. Rev. B **85**, 125204 (2012).
[23]Y. Lee, S. Lee, and G. S. Hwang, Phys. Rev. B **83**, 125202 (2011).
[24]F. Müller-Plathe, J. Chem. Phys. **106**, 6082 (1997).
[25]J. E. Turney, A. J. H. McGaughey, and C. H. Amon, Phys. Rev. B **79**, 224305 (2009).
[26]C. Kittel, *Introduction to Solid State Physics*, 7th ed. (Wiley, New York, 2006).
[27]S. Plimpton, J. Comput. Phys. **117**, 1 (1995).
[28]J. P. Perdew and Y. Wang, Phys. Rev. B **45**, 13244 (1992).
[29]G. Kresse and J. Furthmüller, Phys. Rev. B **54**, 11169 (1996).
[30]J. Che, T. Çagin, and W. A. Goddard, Nanotechnology **11**, 65 (2000).
[31]J. Che, T. Çağın, W. Deng, and W. A. Goddard, J. Chem. Phys. **113**, 6888 (2000).
[32]J.-P. Crocombette and L. Proville, Appl. Phys. Lett. **98**, 191905 (2011).
[33]S. Coffa and S. Libertino, Appl. Phys. Lett. **73**, 3369 (1998).
[34]G. D. Watkins and J. W. Corbett, Phys. Rev. **138**, A543 (1965).
[35]A. La Magna, S. Coffa, and L. Colombo, Phys. Rev. Lett. **82**, 1720 (1999).
[36]A. J. C. Ladd, B. Moran, and W. G. Hoover, Phys. Rev. B **34**, 5058 (1986).
[37]A. J. H. McGaughey and M. Kaviany, Int. J. Heat Mass Transf. **47**, 1783 (2004).
[38]A. J. H. McGaughey and M. Kaviany, Phys. Rev. B **69**, 094303 (2004).